UCRL-JC-123186
PREPRINT

Atomic Structure of the ∑5 (210)/[001] Symmetric Tilt Grain Boundary in Yttrium Aluminum Garnet

Geoffrey H. Campbell
Wayne E. King

This paper was prepared for submittal to the
Ceramic Microstructure '96
Berkeley, CA
June 24, 1996

June 24, 1996

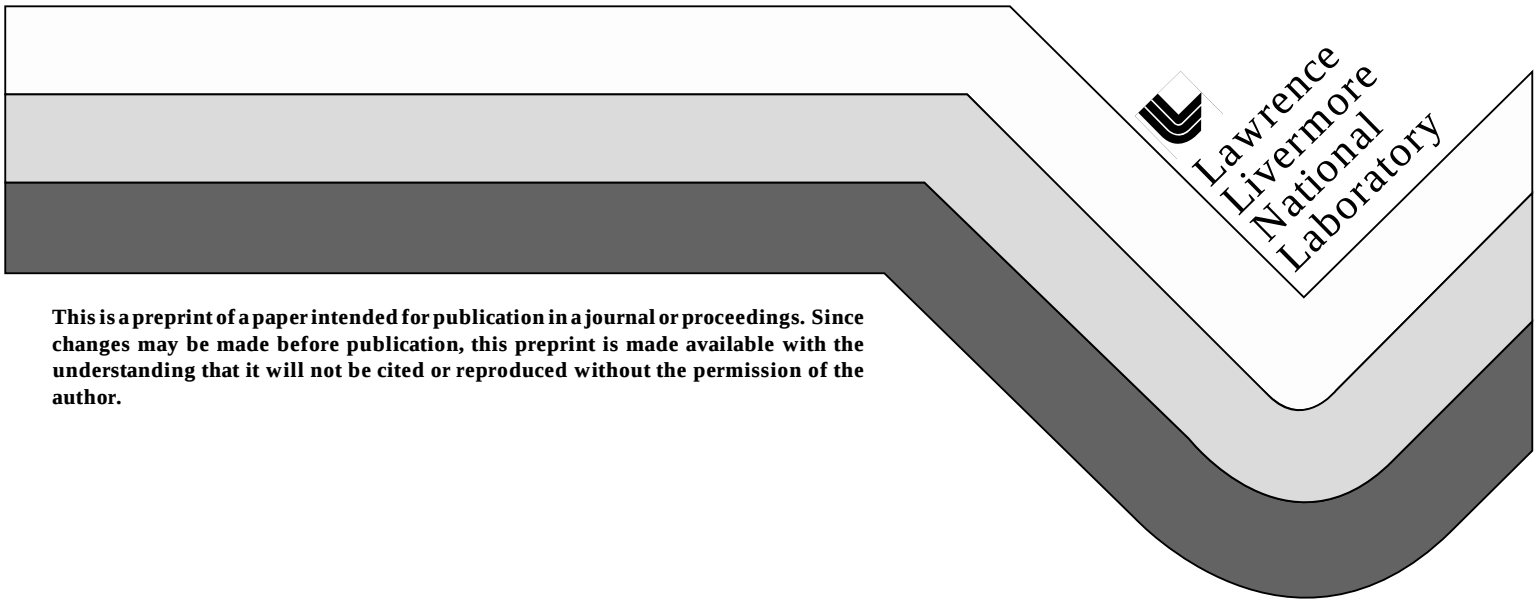

ATOMIC STRUCTURE OF THE ∑5 (210)/[001] SYMMETRIC TILT GRAIN BOUNDARY IN YTTRIUM ALUMINUM GARNET

Geoffrey H. Campbell and Wayne E. King

University of California
Lawrence Livermore National Laboratory
Chemistry and Materials Science Directorate
Livermore, CA 94551

INTRODUCTION

Yttrium aluminum garnet (YAG) is a promising high temperature structural material. Grain boundaries in YAG have been shown to play a critical role in its high temperature behavior. The creep rate of polycrystalline YAG[1] is many orders of magnitude higher than the creep rate of single crystal YAG,[2] indicating that grain boundaries provide a high-diffusivity path for the cations, which facilitates dislocation climb. The contributions of grain boundary sliding and cavitation to the creep rate have not been explicitly investigated and further understanding at the atomic level is required if the high temperature properties are to be controlled.

Atomistic simulations in ceramic materials have been limited compared to those in metals. Commonly, ceramics have comparatively complex crystal structures. For example, the unit cell of YAG contains 160 atoms, even though it is one of the more simple structures with cubic symmetry. Hence, the size of atomistic simulation ensembles are comparatively large, leading to large calculations. Other difficulties are associated with the long range nature of the Coulomb interaction, which causes a slow convergence in summing the contributions to the energy by all the charged ions in the crystal. Whereas in metals the interaction calculation can be cut off after a few nearest neighbors, the ionic interactions must be summed to infinity. Nevertheless, point defect properties of a wide range of ceramics,[3] including YAG,[4] have been calculated. Planar defects have also been simulated in simple oxides and the alkali halides, including surfaces,[5] stacking faults,[6] and grain boundaries.[7, 8]

A limited number of experimental studies of grain boundary atomic structure in ceramics have been performed by high - resolution transmission electron microscopy (HREM), notably in NiO,[9] TiO_2,[10] and Al_2O_3.[11, 12] Comparisons of model predictions to experimental data on the atomic structure of grain boundaries in metals have been very successful in clarifying the limits of some models while providing confirmation of the accuracy of new models.[13] This study will provide relevant experimental data which can readily be compared to the predictions of developmental atomistic models of ceramics. Atomistic simulations with experimentally verified accuracy can be used to develop fundamental understanding of observed material behaviors such as diffusion,[4] which further the understanding of the influence of grain boundaries on the high temperature behavior of YAG.

EXPERIMENTAL METHODS

Materials

Single crystals of pure (undoped) YAG were grown by the Czochralski method and specimens were cut from the lower - stress regions of the boule (Union Carbide Crystal Products, San Diego, CA). Specimens were oriented by Laue x-ray backscatter diffraction and cut into cylinders of 19 mm (0.75 in.) diameter and 12.7 mm (0.5 in.) in length. The faces of the cylinders were cut and polished parallel to the (210) plane to within 0.1°. The faces were polished flat to $\lambda/10$ (55 nm) (Valpey - Fischer Corp., Hopkinton, MA). After the relative rotation relationship was established, a reference flat common to both crystals was ground and polished on the sides of the cylinders in order to re-establish the orientation immediately prior to bonding.[14]

Bonding

The grain boundaries were prepared by ultra - high vacuum (UHV) diffusion bonding.[15] Auger electron spectroscopy (AES) of the as-introduced surface showed carbon as the main surface impurity. Sputtering the surface with 1 keV Xe^+ at a 15° grazing incidence removed the surface contamination to below the detection limit of AES. The rough sides and bottom of the crystals are presumed to remain contaminated after sputtering and thus the crystals were heat treated in UHV at 1200°C for 2h to degas any volatile contamination. Subsequent Auger spectroscopy of the surfaces to be bonded showed no contaminants after annealing.

Immediately prior to bonding, the cleaned surfaces were placed in contact and the crystals were aligned in the twist orientation by reflecting a laser from the reference flat on the sides of the crystals. The alignment was within a reflected spot diameter, which corresponds to approximately 0.1°.

The crystals were bonded with an applied load of 1430 N corresponding to a pressure of 5 MPa and the bonding temperature was 1550°C. The samples were held for six hours at the bonding temperature. During the entire bonding cycle, the total vacuum level never exceeded 1×10^{-5} Pa (7×10^{-8} torr). Residual gas analysis showed H_2 and CO to be the most common residual gases while at temperature.

Characterization by HREM

Specimens for examination in the transmission electron microscope (TEM) were prepared by diamond cutting, polishing, and dimpling. Thinning to final electron transparency was performed by ion milling with 6 keV Ar^+ at 13° grazing incidence. Specimens were lightly coated with carbon to prevent static charging in the microscope.

Two types of specimens where prepared: (i) with the common [001] for both crystals as the specimen normal and (ii) with the common $[1\,\bar{2}\,0]$ as the specimen normal. Both orientations have the grain boundary viewed edge - on. The first is equivalent to viewing the boundary parallel to the tilt axis and the second is viewing the boundary perpendicular to the tilt axis.

Specimens were observed in a high resolution TEM (JEM-4000EX, JEOL, Tokyo, Japan) operating at 400 keV with an objective lens spherical aberration coefficient of 1.0 mm and a spread of focus of 8 nm. Micrographs were acquired on film at an electron - optical magnification of 800 kX with an illumination semi-angle of convergence of 0.91 mrad and an objective aperture diameter equivalent to 13.1 nm^{-1} in reciprocal space.

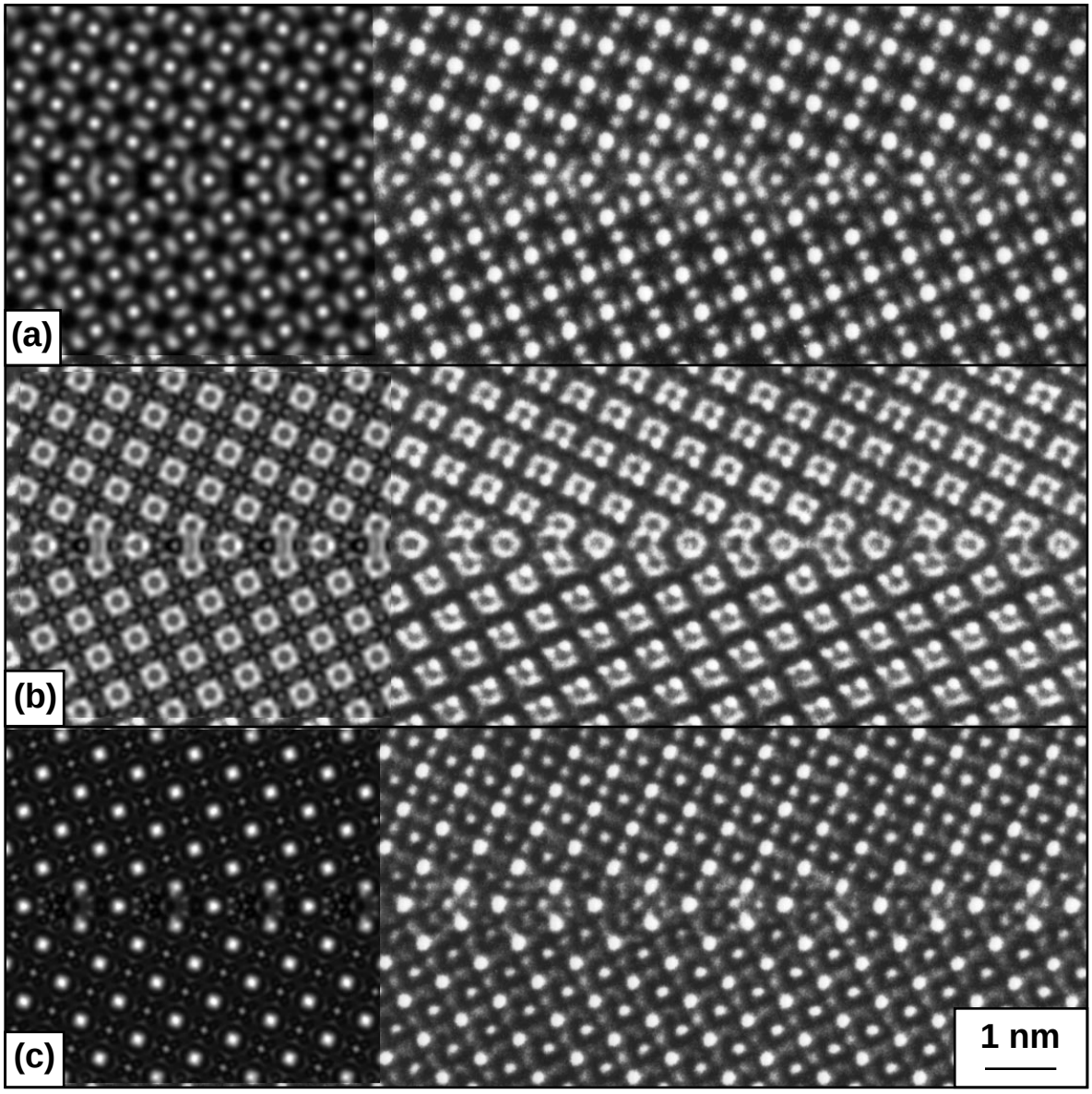

Figure 1. A selection of three micrographs taken of the identical region of a $\Sigma 5$ (210)/[001] symmetric tilt grain boundary in YAG. The images differ only in the microscope focus used to acquire them. The focus deviation values from Gaussian were determined to be (a) 25 nm, (b) -25 nm, and (c) -88 nm. The images are taken along the common [001] direction of the adjacent crystals (parallel to the tilt axis of the boundary). The simulated high resolution images derived from the model structure are shown as inserts on the left.

High Resolution Image Simulation

High resolution image simulation was performed with the EMS suite of computer programs.[16] Crystal structure information was obtained from Wyckoff.[17] Model grain boundary structures were created by simple geometric manipulation of the perfect crystal. This method follows the Coincident Site Lattice model[18] for forming grain boundary structures.

Images of the perfect crystal were calculated by the Bloch wave method with 500 waves included in the calculation. Images of the grain boundary were calculated by the multi-slice technique. The entire repeat unit of the boundary structure was used for each calculation. In the [001] direction the projected potential of four slices of the boundary repeat unit were calculated. In the $[1\,\bar{2}0]$ direction, eight slices were used. The calculation matrix used 190 samples/nm (1024×512 matrix dimensions in [001] and 1024×256 in $[1\,\bar{2}0]$).

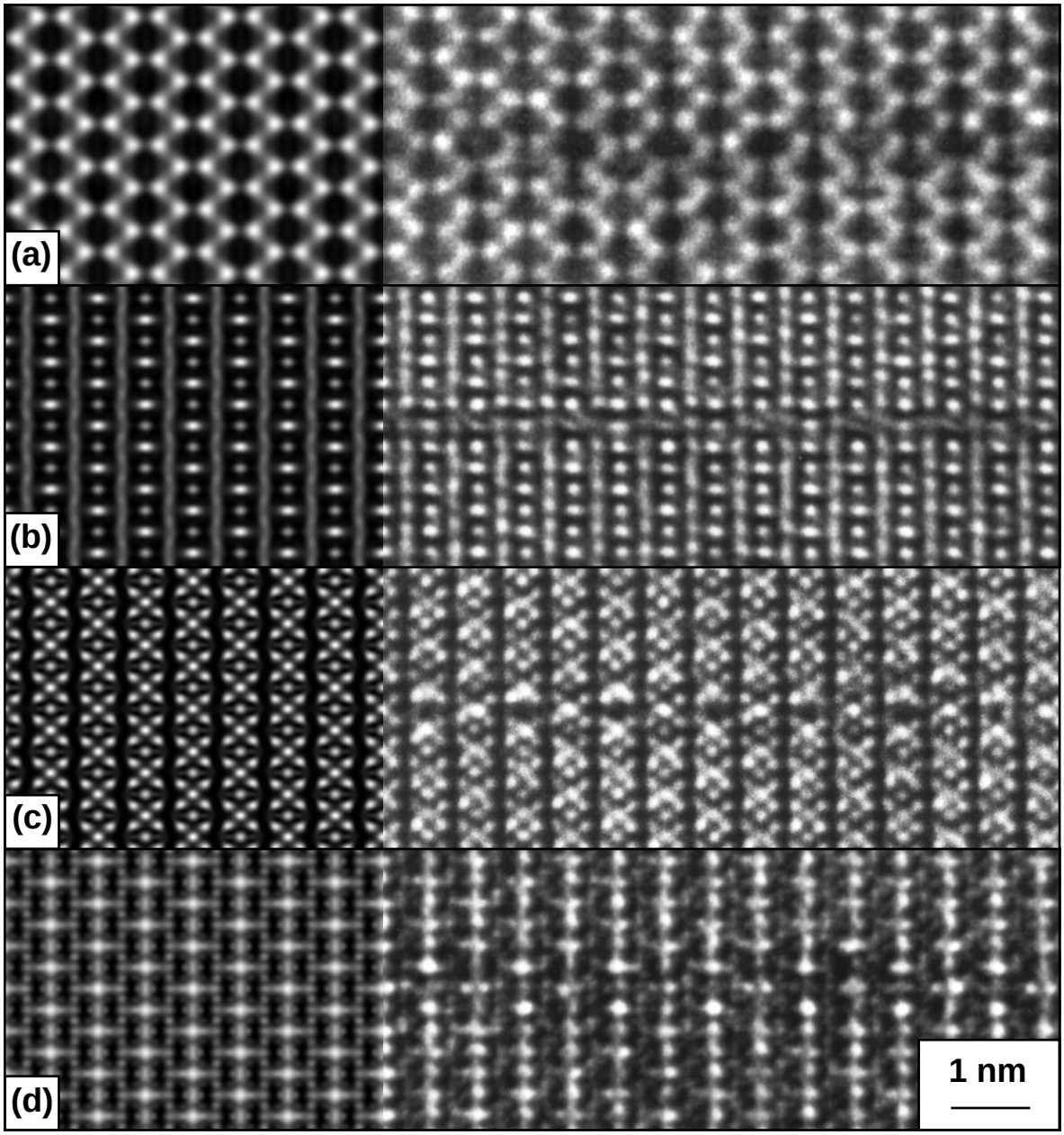

Figure 2. A selection of four micrographs taken of the identical region of a $\Sigma 5$ (210)/[001] symmetric tilt grain boundary in YAG. The images differ only in the microscope focus used to acquire them. The focus deviation values from Guassian were determined to be (a) 65 nm, (b) -5 nm, (c) -60 nm, and (d) -100 nm. The images are taken along the common [1 $\bar{2}$ 0] direction of the adjacent crystals (perpendicular to the tilt axis of the boundary). The simulated high resolution images derived from the model structure are shown as inserts on the left.

RESULTS

Bonding

The diffusion bonded interface produced between the crystals was found to have a small fraction (<1%) of its area decorated with small (~10 μm) residual voids. These voids appeared to be uniformly distributed on the grain boundary. Except for these small voids, bonding was complete across the surface between the crystals even at the edges of the cylinders.

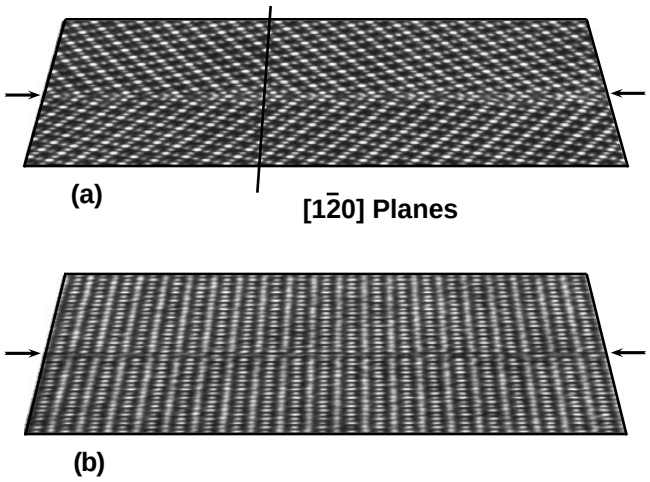

Figure 3. Glancing angle perspective views across the grain boundary using the images seen in (a) Figure 1(a) and (b) Figure 2(b). Due to the distortion, the magnification is not constant across the image, therefore no scale is indicated. The boundary runs horizontally in both cases. It can be seen that the contrast features along the planes perpendicular to the boundary are not displaced when crossing the boundary. A line is drawn in (a) to aid the eye. These images indicate that mirror symmetry of the atomic structure in three dimensions is present at the boundary.

High Resolution Electron Microscopy

Images of the grain boundary were acquired at several values of the microscope focus and at several locations. High resolution images were acquired in both the direction parallel to the tilt axis and perpendicular to the tilt axis. These images are shown in Figures 1 and 2 along with simulated high resolution images as inserts that are discussed in a later section.

The high resolution images can be inspected directly for rigid body translations of the adjacent crystals with respect to one another. The micrographs viewing the boundary parallel to the tilt axis (Figure 3a) show that the crystals are not displaced from a mirror symmetric relation of the crystals to within approximately 0.1 Å. The same holds true for viewing in the direction perpendicular to the tilt axis (Figure 3b). Inspection of the boundary for dilation is more difficult. A first inspection was performed using the technique of Merkle. [19] This technique shows the boundary to be free of dilation to an accuracy of about 0.2 Å.

Atomic Structure and Image Simulation

The garnet crystal is a cubic structure belonging to space group Ia $\bar{3}$d (space-group number 230). It is composed of a body - centered sublattice of Al (octahedrally coordinated sites) with Al - Y pairs on face centers (tetrahedrally coordinated Al and dodecahedrally coordinated Y). The unit cell is composed of 8 formula units, $Y_3Al_5O_{12}$, with a lattice parameter of 1.201 nm. The projection of the unit cell along [001] is shown in Figure 4.

On the basis of the observations of the rigid body displacements, the candidate atomic models can be restricted to only those showing mirror symmetry on the atomic scale about the boundary plane. Inspection of the unit cell of YAG suggests two positions at which the mirror plane can be placed. These planes are indicated in Figure 4. However, simulated HREM images have revealed that only the plane labelled B gives results comparable to the experimental

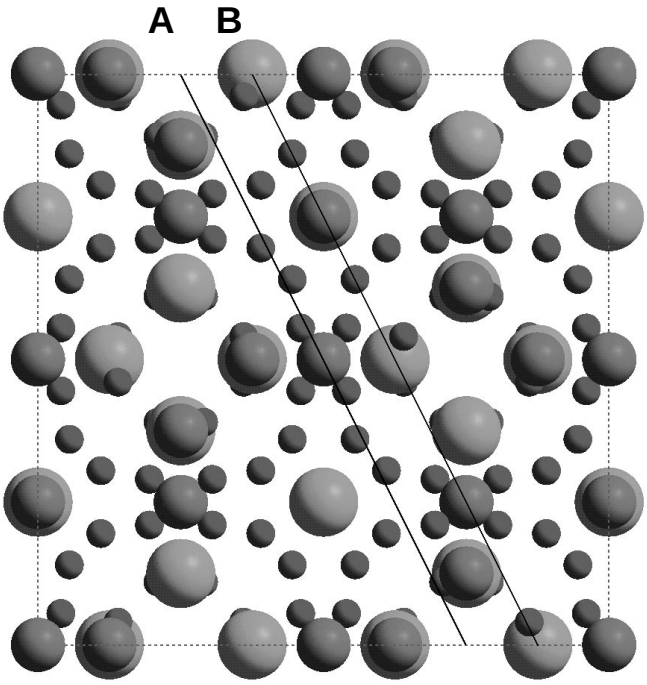

Figure 4. The unit cell of YAG as viewed along [001]. The small spheres are oxygen. The middle - sized spheres are aluminum. The large spheres are yttrium. Two candidate planes for forming the plane of mirror reflection are indicated and labeled A and B.

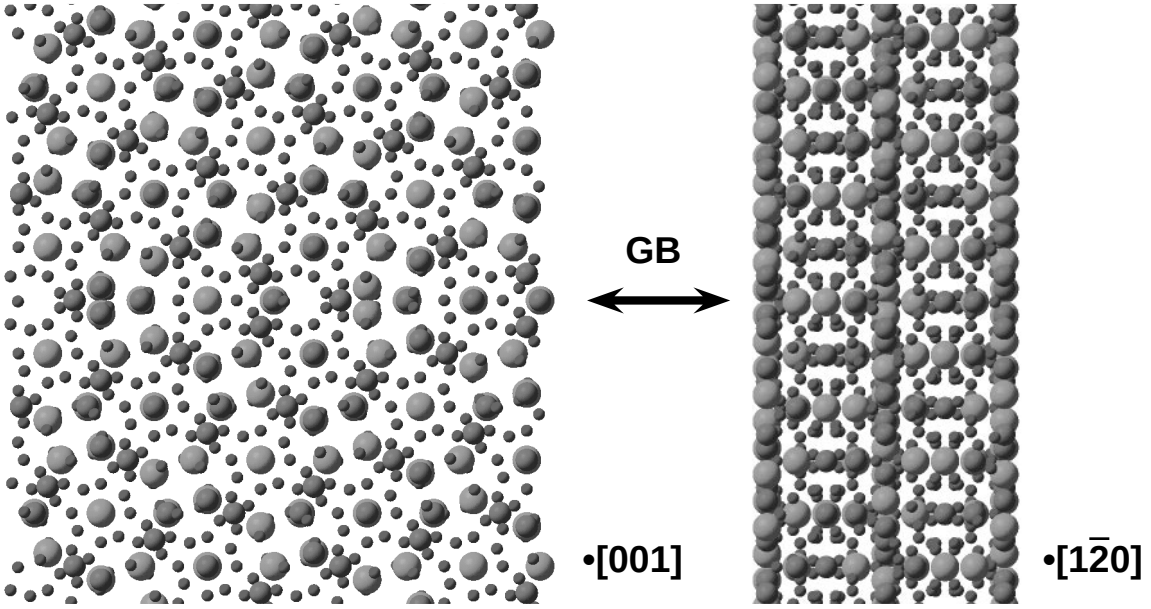

Figure 5. Models of the atomic structure of the ∑5 (210)/[001] symmetric tilt grain boundary in YAG formed by performing a mirror reflection operation at (a) plane A and (b) plane B in Figure 3. One structural unit of the boundary is shown. The plane of the grain boundary is marked by an arrow for each model. The top illustration of the models is a view parallel to the tilt axis along [001] and the bottom illustration is a view perpendicular to the tilt axis along [1 $\bar{2}$0].

images.

The resultant grain boundary structure from performing a twinning operation at plane B is shown in Figure 5. The structural unit of the boundary has a length of 5.370 nm in [1 $\bar{2}$0] and 1.201 nm in [001].

Image simulations for the atomic model are compared with all the experimental images in Figure 1 for viewing along the tilt axis and in Figure 2 for viewing perpendicular to the tilt axis. It is easily seen from this comparison that the grain boundary model agrees reasonably well with the data.

DISCUSSION

The high resolution images show this grain boundary to be atomically flat and straight for extended distances, up to several hundred nanometers. This behavior suggests that the boundary is faceting to a low energy configuration or at least low energy with respect to small deviations from the common (210) crystal plane.

The other remarkable aspect to this boundary is the mirror symmetry exhibited at the atomic scale. Despite examining the boundary at many widely spaced locations and on different TEM specimens, the relative translation state was identical. In all cases, mirror symmetry of atoms on either side of the boundary was found. This behavior is in contrast to that found in NiO,[9] TiO_2,[10] or the fcc metals,[20] where different translational states are observed.

The view of the boundary as projected along the tilt axis clearly shows the twin plane. The structure formed in Figure 5 provides simulated images which closely match the experimental images. The structure of the boundary as projected along [001] is well approximated by the model.

At variance with the view along the tilt axis, the view perpendicular to the tilt axis (Fig. 2) shows a distinct mismatch between the simulated and experimental images of the boundary. In the proposed atomic model, the boundary would be invisible as viewed along [1 $\bar{2}$0]. The boundary is visible in the experimental micrographs. Two possibilities exist for creating the contrast change at the boundary: a change in composition and/or a change in structure. A

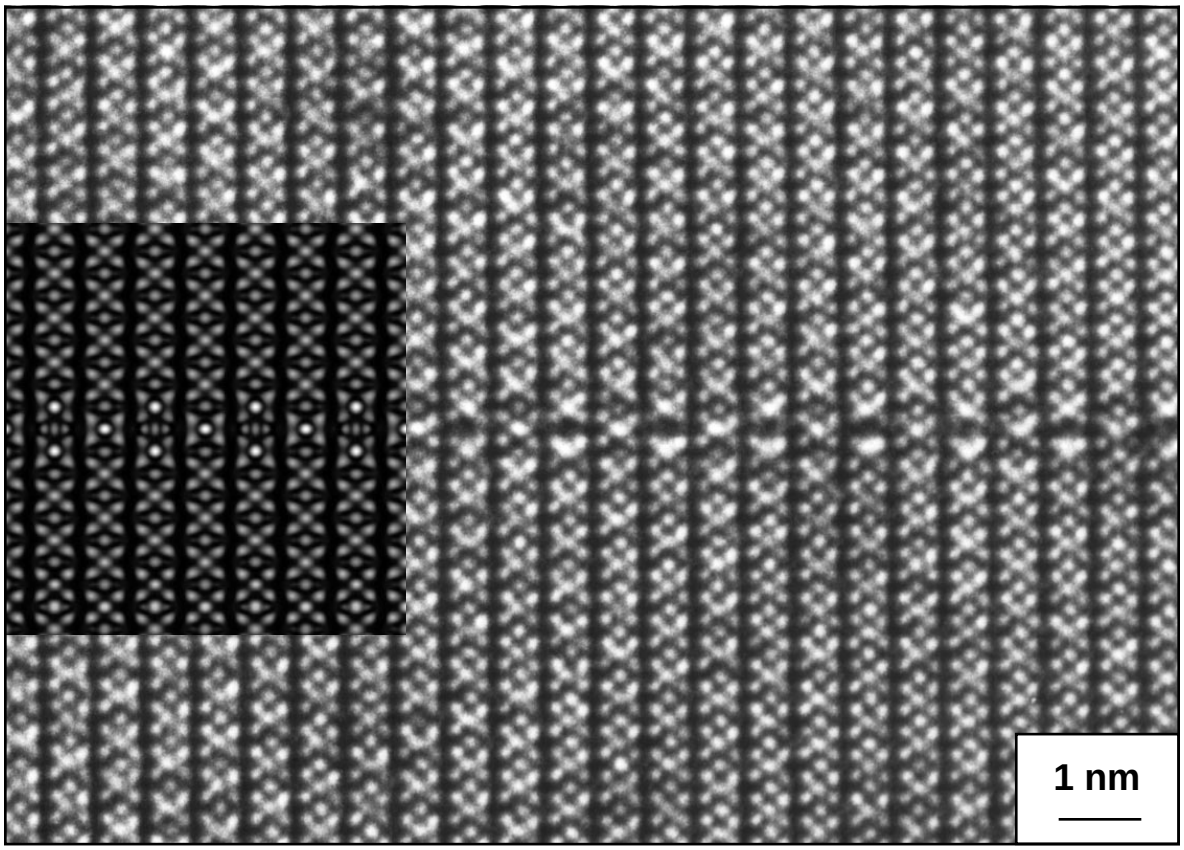

Figure 6. High resolution image simulation using an atomic model whose cation site compositions in the vicinity of the boundary have been altered to bring the simulation into better agreement with the experimental image. The experimental image is the same as that appearing in Figure 1(c).

change in structure would be highly restricted to displacements of atoms in only the [001] direction in order to maintain the image contrast when viewed in projection along [001]. Changing the composition of the boundary could be achieved by replacing Y atoms for Al atoms or vice versa. By changing the cations near the boundary, the contrast from the resulting simulated image can be brought into better agreement with the experimental image (Figure 6). But these changes are made without a physical basis beyond matching the contrast in the simulated and experimental images on a qualitative basis and are thus open to some doubt. In order to achieve a more thorough understanding of the boundary structure, atomistic simulations and more quantitative analysis of the high resolution images[21] would need to be performed to put proposed grain boundary structures on a sound physical basis.

CONCLUSIONS

The $\Sigma 5$ (210)/[001] symmetric tilt grain boundary in YAG was produced by UHV diffusion bonding precisely oriented single crystals. The boundary has been characterized by HREM along two different directions, parallel and perpendicular to the tilt axis. Models of the atomic structure of the boundary were formed following the Coincident Site Lattice scheme. The resulting models are equivalent to twins formed at the atomic scale. The high resolution images show no rigid crystal translations away from the perfect mirror reflection relation. Comparison of the simulated images using the atomic model as input with the experimental images identifies the plane of mirror symmetry. The atomic model is shown to be in good agreement with the experimental images when viewed parallel to the tilt axis, but disagrees with the images perpendicular to the tilt axis. The agreement between the simulated images and the experimental images can be improved by changing the composition of the grain boundary with respect to the bulk. To reach a more certain conclusion on the structure of the grain boundary will require the additional support of theoretical calculations.

ACKNOWLEDGMENTS

We would like to thank John Petrovic for supplying the YAG single crystals. We would also like to thank Ivar Reimanis for stimulating and helpful discussions. We would like to thank Doug Medlin for the use of the 4000EX at Sandia National Laboratories, Livermore. Finally, we would like to thank Walt Wein for his careful work on specimen preparation. This work performed under the auspices of the United States Department of Energy, Office of Basic Energy Sciences and Lawrence Livermore National Laboratory under Contract No. W-7405-Eng-48.

REFERENCES

1. T. A. Parthasarathy, T.-I. Mah and K. Keller, Creep Mechanism of Polycrystalline Yttrium Aluminum Garnet, *J. Am. Ceram. Soc.* 75:1756 (1992).
2. G. S. Corman, Creep of Yttrium Aluminium Garnet Single Crystals, *J. Mater. Sci. Lett.* 12:379 (1993).
3. C. R. A. Catlow and W. C. Mackrodt. *Computer Simulation in Solids*, Springer Verlag, Berlin (1982).
4. L. Schuh, R. Metsalaar and C. R. A. Catlow, Computer Modelling Studies of Defect Structures and Migration Mechanisms in Yttrium Aluminium Garnet, *J. Eur. Ceram. Soc.* 7:67 (1991).
5. P. W. Tasker, The Surface Energies, Surface Tensions and Surface Structure of the Alkali Halide Crystals, *Philos. Mag. A* 39:119 (1979).
6. P. W. Tasker and T. J. Bullough, An Atomistic Calculation of Extended Planar Defects in Ionic Crystals, Application to Stacking Faults in the Alkali Halides, *Philos. Mag. A* 43:313 (1981).
7. D. M. Duffy and P. W. Tasker, Computer Simulation of <001> Tilt Grain Boundaries in Nickel Oxide, *Philos. Mag. A* 47:817 (1983).
8. D. M. Duffy and P. W. Tasker, Computer Simulation of <011> Tilt Grain Boundaries in Nickel Oxide, *Philos. Mag. A* 48:155 (1983).
9. K. L. Merkle and D. J. Smith, Atomic Structure of Symmetric Tilt Grain Boundaries in NiO, *Phys. Rev. Lett.* 59:2887 (1987).
10. U. Dahmen, S. Paciornik, I. G. Solorzano and J. B. Vandersande, HREM Analysis of Structure and Defects in a $\Sigma 5$ (210) Grain Boundary in Rutile, *Interface Sci.* 2:125 (1994).
11. T. Höche, P. R. Kenway, H.-J. Kleebe, M. Rühle and P. A. Morris, High - Resolution Transmission Electrom Microscopy Studies of a Near $\Sigma 11$ Grain Boundary in α - Alumina, *J. Am. Ceram. Soc.* 77:339 (1994).
12. F.-R. Chen, C.-C. Chu, J.-Y. Wang and L. Chang, Atomic Structure of $\Sigma 7(0112)$ Symmetrical Tilt Grain Boundaries in α - Al_2O_3, *Philos. Mag. A* 72:529 (1995).
13. G. H. Campbell, S. M. Foiles, P. Gumbsch, M. Rühle and W. E. King, Atomic Structure of the (310) Twin in Niobium: Experimental Determination and Comparison to Theoretical Predictions, *Phys. Rev. Lett.* 70:449 (1993).
14. W. L. Wien, G. H. Campbell and W. E. King, Preparation of Specimens for Use in Fabricating Bicrystals by UHV Diffusion Bonding, in: *Microstructural Science*, D. W. Stevens, E. A. Clark, D. C. Zipperian and E. D. Albrecht, ed., ASM International, Materials Park, OH (1996).
15. W. E. King, G. H. Campbell, A. W. Coombs, G. W. Johnson, B. E. Kelly, T. C. Reitz, S. L. Stoner, W. L. Wien and D. M. Wilson, Interface Science of Controlled Metal/Metal and Metal/Ceramic Interfaces Prepared Using Ultrahigh Vacuum Diffusion Bonding, in: *Joining and Adhesion of Advanced Inorganic Materials*, A. H. Carim, D. S. Schwartz and R. S. Silberglitt, ed., Materials Research Society, Pittsburgh, PA (1993).
16. P. A. Stadelmann, EMS - A Software Package for Electron Diffraction Analysis and HREM Image Simulation in Materials Science, *Ultramicroscopy* 21:131 (1987).
17. R. W. G. Wyckoff. *Inorganic Compounds $R_x(MX_4)_y$, $R_x(M_nX_p)_y$, Hydrates and Ammoniates*, Interscience Publishers, New York (1965).
18. W. Bollmann. *Crystal Defects and Crystalline Interfaces*, Springer - Verlag, Berlin (1970).
19. K. L. Merkle, Quantification of Atomic - Scale Grain Boundary Parameters by High - Resolution Electron Microscopy, *Ultramicroscopy* 40:281 (1992).
20. D. L. Medlin, M. J. Mills, W. M. Stobbs, M. S. Daw and F. Cosandey, HRTEM Observations of a $\Sigma = 3$ {112} Bicrystal Boundary in Aluminum, in: *Atomic - Scale Imaging of Surfaces and Interfaces*, D. K. Biegelsen, D. J. Smith and S. Y. Tong, ed., Materials Research Society, Pittsburgh, PA (1993).
21. W. E. King and G. H. Campbell, Quantitative HREM Using Non-linear Least-squares Methods, *Ultramicroscopy* 56:46 (1994).